

A signature index for third order topological insulators

L.B Drissi^{1,2,3} and E.H Saidi^{1,2}

1- LPHE, Modeling & Simulations, Faculty of Science, Mohammed V University, Rabat, Morocco.

2- CPM, Centre of Physics and Mathematics, Mohammed V University in Rabat, Morocco.

3- Peter Grünberg Institut and Institute for Advanced Simulation,
Forschungszentrum Jülich & JARA, D-52425 Jülich, Germany.

July 8, 2022

Abstract

In this work, we develop an index signature characterising the third order topological phases in 3D systems. This index is an alternating sum of monomial signatures of Higgs triplet values at 3D corners. We extend our method to N-dimensional systems with open boundaries, and demonstrate that the topological invariant can be efficiently generalised to any space dimension including the second order topological insulators. Known results on lower dimensional systems are recovered and an interpretation in the Higgs space parameters is given.

Keys words: BBH lattice models; Second and Third Order topological Insulators; Index theorem; Higgs space.

1 Introduction

Recently, a new family of topological insulators (HOTIs) going beyond the standard Altland-Zirnbauer (AZ) classification [1, 2] has been discovered by Benalcazar- Bernevig- Hughes (BBH) [3, 4]; see also [5, 6] for related works. Higher Order Topological Insulators —HOTIs— essentially concern the set of 2D and 3D matter systems exhibiting gapless modes at sub-regions of dimensions less or equal to $D - 2$. In 2D systems, with polygonal shapes including the square and the rectangle to be revisited in this study, Second Order Topological Insulators (SOTIs) are characterized by gapless states existing only at corners while the surface and the edges are gapped [7–13]. For 3D matter however; one distinguishes two kinds of HOTIs, namely (i) a second topological order phase on the 1-dimensional edges associated with a periodic boundary condition in z-direction while x- and y- dimensions are open [5]; and (ii) TOTIs; a Third Order Topological Insulator for the point vertices associated with full open boundaries [14]; this third order topological phase concerns 3D poly-faces hosting gapless states at corners (intersections of three 2D faces); while the bulk and the boundary surface as well as their edge intersections are all of them gapped. So far, TOTIs were constructed on the breathing Pyrochlore lattice where each corner of the tetrahedron carries $1/4$ fractional charge [16]. Hall conductance quantized in units of e^2/h was reported for reflection symmetric second-order topological crystalline insulators where the existence of edge states is ensured as long as surface and bulk remain gapped [17]. Gapless corner states were observed experimentally in a two-dimensional quadrupole

topological insulator implemented using perturbative mechanical metamaterials [18]. It was reported in [19] that a realization of TOTIs was explored in an anisotropic diamond- lattice acoustic metamaterial; the bulk acoustic band structure has nontrivial topology characterized by quantized Wannier centers. By acoustic measurement, gapless states were observed at two corners of a rhombohedron- like structure in agreement with non trivial topology characterized by quantized Wannier centers [20].

Topological invariants are so important for a more comprehensive classification of topological crystalline insulators [4,21]. Remarkably, this notion encodes information on the boundary physics and provides access to natural quantities and observables [22–24]. A noninteracting \mathbb{Z}_2 topological invariant was given in term of the Berry curvature for topological insulators (TIs) [25]. For interacting and disordered TI systems, topological index, that determines their phase diagrams, can be experimentally measured through the topological magneto-electric effect [26–28]. For suitable types of noise, the classification of mixed-state topology in one dimension reveals retainment of its topological properties [29]. Furthermore, topological Thouless pump is induced by Markovian reservoirs in open quantum chains [30]. The integer invariant describing the topology of 2D open systems captures the number difference of gapless edge modes and gapless edge blind bands [31]. Remarkably, in the limit of TIs, topological invariants are well investigated, however, they are not perfectly developed and are to be described for HOTIs.

In this paper, we derive an explicit formula for the topological invariant characterising TOTIs in 3D parallelepiped systems with the cube as a particular case. For that, we consider the topological DBI class of the AZ periodic table which has reflection symmetries, in addition to the usual T- P- C invariance. These kind of systems have full open boundary conditions with topological dynamics remarkably described by the limits of the lattice Hamiltonian near the Dirac points. It happens that the resulting limits can be interpreted in terms of couplings between fermions and scalar fields as done in [34]; and to which we refer below to as Fukui- coupling. This nice observation has in fact a deep origin since from the quantum field theory view (QFT), the coupling can be put in a *formal correspondence*¹ with the well known Yukawa tri-coupling $\psi^\dagger \phi \psi$ giving masses to fermions through a non zero vacuum expectation value $\langle \phi \rangle$ of the Higgs field ϕ ; the fields ψ and ψ^\dagger describes the fermionic states. Borrowing this idea and applying it to 3D lattice systems, we develop the topological picture for 3-dimensional BBH system and show amongst others that the underlying topological index $Ind(H_{3D})$ is given by

$$Ind(H_{3D}) = \sum_{p,q,s=\pm} \frac{pq s}{8} sgn(A_p B_q C_s) \quad (1.1)$$

with A_\pm, B_\pm, C_\pm are non vanishing constants whose meaning may be imagined in terms of vacuum expectation values of an O(3) scalar (Higgs) field triplet (ϕ_x, ϕ_y, ϕ_z) . These constants are the values of Higgs field at space infinities; they will be discussed in details in the heart of the paper. We also show that the above index formula has a remarkable factorisation as in Eq.(4.38) showing in turns that $Ind(H_{3D})$ is just an element of a sequence with a generic term as follows

$$Ind(H_{ND}) = \prod_{i=1}^N \left[\sum_{p_i=\pm} \frac{p_i}{2} sgn(A_{p_i}) \right] \quad (1.2)$$

By setting $N = 3$, we recover exactly the index formula (1.1); for $N = 1$, one obtains an index formula for the 1-dimensional Su- Schrieffer- Heeger models (SSH) model [33] which reads here as $\frac{1}{2}(sgn A_+ - sgn A_-)$;

¹ This correspondence is purely formal; it is used here to emphasize the role played by the scalar field ϕ in our calculations. Clearly this ϕ is not the true Higgs scalar field of the standard model of elementary particles. There, the Higgs field is a complex field doublet; it has a scalar potential $\mathcal{V}(h) = -\mu^2 |h|^2 + \lambda |h|^4$ having a non trivial minimum $h_{\min} \neq 0$. Moreover, the h couples to several fields of the model; in particular to fermions like $\psi^\dagger h \psi$. In our present study, the ϕ scales in same manner as h and has a quite similar tri-coupling $\psi^\dagger \phi \psi$. Here, the ϕ is handled as in [34].

and by setting $N = 2$, we discover the Fukui formula for $Ind(H_{2D})$ describing the second order topological systems of 2D matter systems. This 2D index formula can be expressed like $\sum_{p,q=\pm} \frac{pq}{2} \text{sgn}(A_p B_q)$; it is also factorable like

$$Ind(H_{2D}) = \frac{1}{2} [\text{sgn}(A_+) - \text{sgn}(A_-)] \times \frac{1}{2} [\text{sgn}(B_+) - \text{sgn}(B_-)] \quad (1.3)$$

and remarkably descends for the 3-dimensional index formula $Ind(H_{3D})$ by fixing the C_{\pm} signatures of the third component ϕ_z of the Higgs field triplet as $\text{sgn}(C_+) = +1$ and $\text{sgn}(C_-) = -1$.

The organisation of this paper is as follows: In section II, we revisit some useful aspects of the 2D model with full open boundary conditions and compute the topological index $Ind(H_{2D})$ by using two different methods that will be commented at proper places; the one used by Fukui and an equivalent one using the power of differential forms. In section III, we shed more light on the derivation of the Fukui formula by using a direct approach based on topological mappings. In section IV, we develop the construction to 3-dimensions and show that the topological index $Ind(H_{3D})$ for the third order topological phase in DBI class with reflection symmetries is given by Eq(1.1). Section V is devoted to conclusion and comments. In the appendices A and B, we report some technical details which have been omitted from the core of the paper in order to keep the chain of ideas forward to the index derivation.

2 Two dimensional BBH model revisited

Following [34], the index of the Hamiltonian —Ind(H)— of the two dimensional BBH lattice model with open boundary conditions can be determined by studying the properties of a $2 + 2$ component fermion $\psi = (\lambda, \chi)$ near the four Dirac-like points $\mathbf{k}_{\mathbf{n}\pi}^*$ of the model which are equal to $(n_x\pi, n_y\pi)$ with $n_i = 0, 1$; see details given after Eq(2.1) and further details in appendix A. Around each one of these $\mathbf{k}_{\mathbf{n}\pi}^*$ points, the fermion ψ is coupled to an external 2D vector $\varphi_{\mathbf{n}\pi}$ with constant components $(\varphi_{n_x\pi}^x, \varphi_{n_y\pi}^y)$, thus playing the role of a mass — i.e: a gap energy between valence and conducting bands—. We refer below to this $\varphi_{\mathbf{n}\pi}$ as constant $O(2)$ Higgs field doublet; its two components $\varphi_{n_a\pi}^a$ depend on the Dirac point on which one rests; they are given by $\Delta_a + \cos(n_a\pi)$ where Δ_x and Δ_y are hopping parameters of the model. For example, near the Dirac point $n_x = n_y = 0$, the Higgs components φ_0^x and φ_0^y read respectively like $\Delta_x + 1$ and $\Delta_y + 1$; while near another point, say $n_x = 0, n_y = \pi$, we have $(\varphi_0^x, \varphi_\pi^y)$ with y-component like $\Delta_y - 1$. So, given a Dirac point, the interacting dynamics between fermion ψ , its adjoint ψ^\dagger and the Higgs field is described by the following typical Hamiltonian matrix

$$H = \mathbf{\Lambda}^x k_x + \mathbf{\Lambda}^y k_y + \mathbf{\Omega}^x \varphi_x + \mathbf{\Omega}^y \varphi_y \quad (2.1)$$

where the hermitian 4×4 matrices $\mathbf{\Lambda}^i$ and $\mathbf{\Omega}^i$ and their basic properties will be specified below. To fix ideas, the term $\mathbf{\Lambda}^x k_x + \mathbf{\Lambda}^y k_y$ may be viewed as the leading contribution coming from the expansion of $\mathbf{\Lambda}^x \sin k_x + \mathbf{\Lambda}^y \sin k_y$ near the Dirac point $(k_x, k_y) = (0, 0)$ while the terms $\mathbf{\Omega}^x \varphi_x$ and $\mathbf{\Omega}^y \varphi_y$ derive from the expansion of $\mathbf{\Omega}^x (\Delta_x + \cos k_x)$ and $\mathbf{\Omega}^y (\Delta_y + \cos k_y)$ respectively [3, 4]. In appendix A, we show that the above H is in fact a representative of a set of four Hamiltonians $H_{n_x\pi, n_y\pi}$ obtained by the expansions of an underlying lattice H_{lat} near the points $(k_x, k_y) = (n_x\pi, n_y\pi)$ with $n_x, n_y = 0, 1 \bmod 2$. Notice by the way that the denomination of the usual four matrices γ^μ of Dirac theory by the pairs $\mathbf{\Lambda}^i$ and $\mathbf{\Omega}^i$ is for convenience; it will be justified later on. Observe also that, in addition to the 2D momentum vector variables (k_x, k_y) , Eq(2.1) depends also on the constant (φ_x, φ_y) that can be interpreted at this level as moduli parameters and whose role they play will be explored during this study. Notice as well that H has discrete symmetries given by the basic T - P - C invariance of AZ classification [1, 2] and moreover

by mirror symmetries going beyond AZ. The basic symmetries, respectively generated by time reversing symmetry (TRS) operator \mathbf{T} , particle-hole \mathbf{P} and chiral operator \mathbf{C} , act on H as follows

$$\begin{aligned} \mathbf{T}H(k_x, k_y)\mathbf{T}^{-1} &= +H(-k_x, -k_y) \\ \mathbf{P}H(k_x, k_y)\mathbf{P}^{-1} &= -H(-k_x, -k_y) \\ \mathbf{C}H(k_x, k_y)\mathbf{C}^{-1} &= -H(k_x, k_y) \end{aligned} \quad (2.2)$$

The obey the characteristics of the DBI class and are realised like: $\mathbf{T} = K$ with K standing for the usual $(*)$ complex conjugation; $\mathbf{C} = \gamma_5$ for chirality and \mathbf{P} given by the composed operator $\gamma_5 K$. Regarding the mirror symmetries, they are generated by the \mathbf{M}_x and \mathbf{M}_y reflections in the x- and y- directions operating as follows

$$\begin{aligned} \mathbf{M}_x H(k_x, k_y)\mathbf{M}_x^{-1} &= H(-k_x, k_y) \\ \mathbf{M}_y H(k_x, k_y)\mathbf{M}_y^{-1} &= H(k_x, -k_y) \\ \mathbf{M}_{xy} H(k_x, k_y)\mathbf{M}_{xy}^{-1} &= H(-k_x, -k_y) \end{aligned} \quad (2.3)$$

with $\mathbf{M}_{xy} = \mathbf{M}_y \mathbf{M}_x$ for inversion. The two \mathbf{M}_j operators are realised by $i\mathbf{\Lambda}_j \gamma_5$ and capture important properties [17]; they commute with \mathbf{T} but anticommutes with γ_5 ; the last property prevents a γ_5 term in H . So, by requiring these reflection symmetries, the above time reversing invariant Dirac Hamiltonian H has inevitably chiral symmetry which is at the basis of our following calculations. Recall that the gap energy of (2.1) is induced by the constant φ ; gapless states require then the vanishing of φ . In the remainder of the paper, we think of the topological nature of the corner states of same type as the Jackiw- Rossi states [35]; for that we promote the constant φ^a to a smooth space coordinate dependent $\phi^a = \phi^a(x, y)$ with topological transition encoded by a sign change of the Higgs field ϕ^a . In what follows, we substitute (2.1) by the relaxed Hamiltonian $\mathbf{\Lambda}^i k_i + \mathbf{\Omega}^a \phi_a$ where ϕ^a is coordinate dependent and summation over repeated indices. Regarding materials, notice that our present work concerns solids with corners and boundary edges related by reflection symmetries; and so the results to be derived below apply to those 2D- and 3D-materials having discrete symmetry groups \mathcal{G}_{2D} and \mathcal{G}_{3D} containing reflections as sub-symmetries.

2.1 Integral formula for $\text{Ind}(H)$

To characterise the topological properties of (2.1) captured by gapless states at corners of the rectangular system, we use chiral symmetry \mathbf{C} of the model to calculate the index of the hamiltonian; this is achieved by applying the method of [34] relying on the fermion-Higgs coupling to reach $\text{Ind}(H)$. For this purpose, let us begin by giving some useful tools to fix ideas and which are also helpful when studying the 3D system. The four energy bands of H are described by $2 + 2$ component fermion $\psi = \psi(x, y)$ that we split like

$$\psi = \begin{pmatrix} \lambda \\ \bar{\chi} \end{pmatrix} \quad (2.4)$$

with $\bar{\chi} = \chi^*$ and where

$$\lambda = \begin{pmatrix} \lambda_1 \\ \lambda_2 \end{pmatrix}, \quad \chi = \begin{pmatrix} \chi_1 \\ \chi_2 \end{pmatrix} \quad (2.5)$$

The explicit form of the wave functions describing gapless states at each corner are obtained by solving the two following constraint relations:

1. The eigenvalue equation $H\psi = E\psi$ with energy $E = 0$ and local hamiltonian as

$$H = -i\mathbf{\Lambda}^j \frac{\partial}{\partial x^j} + \mathbf{\Omega}^a \phi_a \quad (2.6)$$

where we have used $k_j = -i \frac{\partial}{\partial x^j}$. Here, the matrices $\mathbf{\Lambda}^j$ and $\mathbf{\Omega}^a$ are realised in terms of two sets of Pauli matrices $\boldsymbol{\sigma}$ and $\boldsymbol{\tau}$ as follows

$$\begin{aligned} \mathbf{\Lambda}_1 &= \tau_2 \otimes \sigma_1 & , & & \mathbf{\Lambda}_2 &= \tau_2 \otimes \sigma_3 \\ \mathbf{\Omega}_1 &= \tau_2 \otimes \sigma_2 & , & & \mathbf{\Omega}_2 &= \tau_1 \otimes \sigma_0 \end{aligned} \quad (2.7)$$

with the properties $T\mathbf{\Lambda}_i T^{-1} = -\mathbf{\Lambda}_i$ and $T\mathbf{\Omega}_a T^{-1} = \mathbf{\Omega}_a$ while $C\mathbf{\Lambda}_i C^{-1} = -\mathbf{\Lambda}_i$ and $C\mathbf{\Omega}_a C^{-1} = -\mathbf{\Omega}_a$. The $\mathbf{\Lambda}_i$ and $\mathbf{\Omega}_a$ matrices square to identity and anticommute among themselves; for a generic description of these matrices; it is interesting to set $\mathbf{\Lambda}_1 = \gamma_1, \mathbf{\Omega}_1 = \gamma_2$ and $\mathbf{\Lambda}_2 = \gamma_3, \mathbf{\Omega}_2 = \gamma_4$; by using these γ_μ 's, the underlying 4-dim Euclidian Clifford algebra reads as $\gamma_\mu \gamma_\nu + \gamma_\nu \gamma_\mu = 2\delta_{\mu\nu}$ and the chiral operator is given by $\gamma_5 = -\gamma_1 \gamma_2 \gamma_3 \gamma_4$; it represents the C in Eq.(2.2) and defines chirality of the states. As given below, chiral and antichiral fermions have the half degrees of freedom carried by ψ ,

$$\gamma_5 \begin{pmatrix} \lambda \\ 0 \end{pmatrix} = - \begin{pmatrix} \lambda \\ 0 \end{pmatrix} \quad , \quad \gamma_5 \begin{pmatrix} 0 \\ \bar{\chi} \end{pmatrix} = \begin{pmatrix} 0 \\ \bar{\chi} \end{pmatrix} \quad (2.8)$$

2. A chirality condition, killing the half of the components of ψ , is given by the equation

$$\gamma_5 \psi = q_\gamma \psi \quad , \quad \gamma_5 = -\tau_3 \otimes \sigma_0 \quad (2.9)$$

The chiral charge q_γ takes either the value $+1$ or -1 ; the exact value of this charge at corner is fixed by the normalisation condition of $\psi(\mathbf{r})$. By taking ϕ_a positive constants for instance, the ψ is given by a real exponential $e^{-\boldsymbol{\kappa} \cdot \mathbf{r}}$ with momentum $\boldsymbol{\kappa}$ which is function of q_γ ; by demanding $\boldsymbol{\kappa} \cdot \mathbf{r} > 0$, one ends with a constraint on the sign of the chiral charge; see [38] for details.

After this digression on ψ and the algebra of the $\mathbf{\Lambda}^j$ and $\mathbf{\Omega}^a$ matrices, we come now to the study of the index of Hamiltonian H ; this index can be expressed in different, but equivalent, ways. The standard definition is given by the integer

$$Ind(H) = N_+ - N_- \quad (2.10)$$

with N_\pm standing for the numbers of chiral and antichiral zero modes in the ground state. To compute the value of this index, it is helpful to take advantage of two interesting features: First, we think of this integer as the flux of some two dimensional current $J^i = J^i(\mathbf{r})$ as follows

$$Ind(H) = \oint_{\mathcal{C}} \varpi \quad \text{with} \quad \varpi = \frac{1}{2} (J^x dy - J^y dx) \quad (2.11)$$

with closed contour \mathcal{C} belonging to the x-y plane. Below, we refer to this position plane as $\mathbb{R}_{\mathbf{r}}^2$ and so the loop \mathcal{C} sits in $\mathbb{R}_{\mathbf{r}}^2$; the reason for this notation is that we will encounter below another closed curve Γ belonging to another plane \mathbb{R}_{ϕ}^2 parameterised by the $\phi = (\phi_x, \phi_y)$ components of the Higgs field doublet. By using the antisymmetric Levi-Civita symbol ε^{ij} and its inverse ε_{ji} with $\varepsilon^{12} = \varepsilon_{21} = 1$, the above index reads in a generic form like

$$Ind(H) = -\frac{1}{2} \oint_{\mathcal{C}} J^i (\varepsilon_{ij} dx^j) . \quad (2.12)$$

showing that $Ind(H)$ is indeed the flux of the J_i vector. Second, we interpret the vector current J^i as the vacuum expectation value (VEV) of an axial vector current J_5^i involving the matrix operator γ_5 generating chirality. In other words, we have $J^i = \langle J_5^i \rangle$ reading in terms of the Hamiltonian H (2.1-2.6) as follows [34, 38–42],

$$J^i(\mathbf{r}) = \lim_{\mathbf{r}' \rightarrow \mathbf{r}} \left[\lim_{m \rightarrow 0} tr \left(\gamma_5 \mathbf{\Lambda}^i \frac{1}{m + iH} \right) \delta_2(\mathbf{r} - \mathbf{r}') \right] . \quad (2.13)$$

By calculating the trace over the 4×4 matrix product in (2.13) and taking the vanishing mass limit, the above vector current can be expressed in terms of the Higgs field as follows

$$J^i = \frac{1}{\pi |\phi|^2} \varepsilon^{ij} \phi_a \partial_j \phi_b \varepsilon^{ab}. \quad (2.14)$$

with $|\phi|^2 = \phi_x^2 + \phi_y^2$. The derivation of Eq.(2.14) is somehow technical; a sketch of its obtention is reported in appendix B. By substituting this current vector back into (2.12), we end up with the following integral formula

$$\text{Ind}(H) = \oint_{\mathcal{C}} \frac{1}{2\pi |\phi|^2} \varepsilon^{ab} \phi_a \partial_j \phi_b dx^j \quad (2.15)$$

This relation shows that $\text{Ind}(H)$ is intimately related with the Higgs fields; thank to fermion-Higgs coupling which allowed to extract the ground state data $N_+ - N_-$.

2.2 Signature formula for $\text{Ind}(H)$

To calculate $\text{Ind}(H)$, we must perform the integral in (2.15) which can be interpreted as a function $\mathcal{F}[\mathcal{C}]$ with variable given by an extended object namely the loop \mathcal{C} . For that, we a priori have to specify the closed curve \mathcal{C} in order to get the numerical value of $\text{Ind}(H)$. In fact, this is not necessary since $\text{Ind}(H)$ is a topological invariant and so it is non sensitive to the shape of \mathcal{C} ; we will use this property later on in order to re-derive the result of [34]. Before that, let us follow the Fukui approach by thinking of the curve in Eq.(2.15) as a big closed \mathcal{C}_∞ at the boundary of the x-y plane; and moreover imagine it as a rectangular loop $\mathcal{C}_\infty^{(4)}$ with four edges as depicted in the **Figure 1**.

$$\mathcal{C}_\infty^{(4)} = \mathcal{C}_1 \cup \mathcal{C}_2 \cup \mathcal{C}_3 \cup \mathcal{C}_4 \quad (2.16)$$

We also require that at the four corners of the rectangular curve $\mathcal{C}_\infty^{(4)}$, the Higgs components (ϕ_x, ϕ_y) take constant values denoted below like (A_\pm, B_\pm) . In other words, on the boundary edges of $\mathcal{C}_\infty^{(4)}$, the Higgs

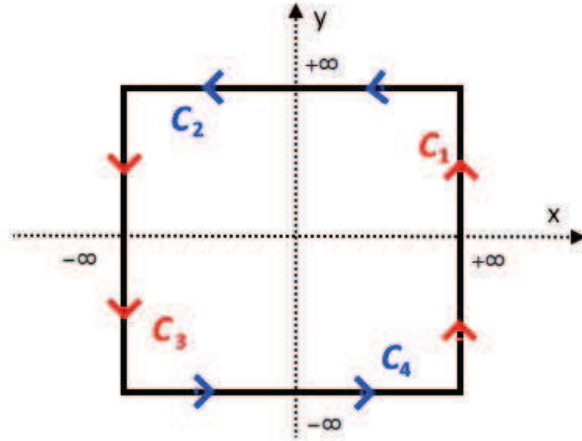


Figure 1: Flux of the vector current through the rectangular boundary at space infinity. This curve choice allows to collect the full flux.

field components satisfy space boundary conditions of the type

$$\begin{aligned} \lim_{x \rightarrow \pm\infty} \phi_x(x, y) &= \phi_x(\pm\infty, y) = A_\pm \\ \lim_{x \rightarrow \pm\infty} \phi_y(x, y) &= \phi_y(\pm\infty, y) = G(y) \end{aligned} \quad (2.17)$$

and

$$\begin{aligned}\lim_{y \rightarrow \pm\infty} \phi_y(x, y) &= \phi_y(x, \pm\infty) = B_{\pm} \\ \lim_{y \rightarrow \pm\infty} \phi_x(x, y) &= \phi_x(x, \pm\infty) = F(x)\end{aligned}\quad (2.18)$$

where A_{\pm} and B_{\pm} are non vanishing constants. We also have $\lim_{x \rightarrow \pm\infty} F(x) = A_{\pm}$ and $\lim_{y \rightarrow \pm\infty} G(y) = B_{\pm}$. This implies that the value of the field components (ϕ_x, ϕ_y) at the corners of the rectangle are precisely given by (A_{\pm}, B_{\pm}) . With these boundary conditions the vector current (2.14) on the curve \mathcal{C}_{∞} becomes

$$\begin{aligned}J^x(x, y)|_{\mathcal{C}_1} dy &= \frac{\varepsilon^{ab}}{\pi(A_+^2 + G^2)} G_a \partial_y G_b dy \\ J^y(x, y)|_{\mathcal{C}_2} dx &= \frac{-\varepsilon^{ab}}{\pi(B_+^2 + F^2)} F_a \partial_x F_b dx\end{aligned}\quad (2.19)$$

that read also like

$$\begin{aligned}J^x(x, y)|_{\mathcal{C}_1} dy &= \frac{1}{\pi} \frac{dg}{1+g^2} \\ J^y(x, y)|_{\mathcal{C}_2} dx &= \frac{1}{\pi} \frac{df}{1+f^2}\end{aligned}\quad (2.20)$$

where we have set $g = \frac{G}{A_+}$ and $f = \frac{F}{B_+}$. Because of the property $\frac{d\xi}{1+\xi^2} = d(\arctan \xi)$, the above $J_x|_{\mathcal{C}_1} dy$ and $J_y|_{\mathcal{C}_2} dx$ are exact 1-forms given by

$$\begin{aligned}J^x(x, y)|_{\mathcal{C}_1} dy &= \frac{1}{\pi} d(\arctan g) \\ J^y(x, y)|_{\mathcal{C}_2} dx &= \frac{1}{\pi} d(\arctan f)\end{aligned}\quad (2.21)$$

Similarly, we have

$$\begin{aligned}J^x(x, y)|_{\mathcal{C}_3} dy &= \frac{1}{\pi} d(\arctan \tilde{g}) \\ J^y(x, y)|_{\mathcal{C}_4} dx &= \frac{1}{\pi} d(\arctan \tilde{f})\end{aligned}\quad (2.22)$$

with $\tilde{g} = \frac{\tilde{G}}{A_-}$ and $\tilde{f} = \frac{\tilde{F}}{B_-}$. Substituting these relations back into Eq. (2.11), and using

$$\begin{aligned}\int_{\mathcal{C}_1} \varpi &= \frac{1}{2\pi} \arctan \frac{B_+}{A_+} - \frac{1}{2\pi} \arctan \frac{B_-}{A_+} \\ \int_{\mathcal{C}_2} \varpi &= \frac{1}{2\pi} \arctan \frac{A_+}{B_+} - \frac{1}{2\pi} \arctan \frac{A_-}{B_+}\end{aligned}\quad (2.23)$$

as well as

$$\begin{aligned}\int_{\mathcal{C}_3} \varpi &= \frac{1}{2\pi} \arctan \frac{B_-}{A_-} - \frac{1}{2\pi} \arctan \frac{B_+}{A_-} \\ \int_{\mathcal{C}_4} \varpi &= \frac{1}{2\pi} \arctan \frac{A_-}{B_-} - \frac{1}{2\pi} \arctan \frac{A_+}{B_-}\end{aligned}\quad (2.24)$$

we end up with the following value of the index

$$\begin{aligned}Ind H &= \frac{1}{2\pi} (\arctan \frac{B_+}{A_+} + \arctan \frac{A_+}{B_+}) - \frac{1}{2\pi} (\arctan \frac{A_-}{B_+} + \arctan \frac{B_+}{A_-}) \\ &\quad - \frac{1}{2\pi} (\arctan \frac{B_-}{A_-} + \arctan \frac{A_-}{B_-}) - \frac{1}{2\pi} (\arctan \frac{A_+}{B_-} + \arctan \frac{B_-}{A_+})\end{aligned}\quad (2.25)$$

Using the relation $\arctan \xi + \operatorname{arccot} \xi = \frac{\pi}{2} \operatorname{sgn}(\xi)$, we can put the above relation into the following form

$$\begin{aligned}Ind(H) &= +\frac{1}{4} [\operatorname{sgn}(A_+ B_+) + \operatorname{sgn}(A_- B_-)] \\ &\quad - \frac{1}{4} [\operatorname{sgn}(A_+ B_-) + \operatorname{sgn}(A_- B_+)]\end{aligned}\quad (2.26)$$

which shows that $Ind(H)$ takes indeed an integer value; this is the Fukui formula [34]. For the example where A_{\pm}, B_{\pm} have the same sign, the index vanishes identically; it vanishes also for other cases like $\operatorname{sgn}(A_{\pm}) = 1$ and $\operatorname{sgn}(B_{\pm}) = -\operatorname{sgn}(B_{\mp})$. However, for the cases A_+, B_+ positive (resp. negative) definite numbers and A_-, B_- negative (resp. positive) definite ones; the index of the Hamiltonian is equal to +1 (resp. -1). For the example $A_- = -A_+$ and $B_- = -B_+$, the index of H reduces to $\operatorname{sgn}(A_+ B_+)$ which can be either +1 or -1 depending on the signs of A_+ and B_+ ; for instance this is the case of $A_+ = B_+$ and $A_+ = -B_+$.

3 More on Ind(H) in 2-dim DBI

In this section, we shed more light of the derivation of the Fukui formula by using a direct approach based on topological mapping between the curve \mathcal{C} in the x-y position space $\mathbb{R}_{\mathbf{r}}^2$ and a corresponding curve Γ in the ϕ_x - ϕ_y Higgs space \mathbb{R}_{ϕ}^2 . We show amongst others that for a non trivial index the $sgn(\phi_x)$ and $sgn(\phi_y)$ have to change their polarity under space reflections.

3.1 Working in Higgs plane

The index formula (2.26) obtained by using the curve choice (2.16) is remarkable and suggestive; it involves only $sgn(X)$ functions in agreement with the topological aspect of the index; it is given by the sum of four terms; each contributing with $\pm\frac{1}{4}$ and add exactly to an integer. This relation shows that the four terms in (2.26) are in one to one correspondence with the four (A_{\pm}, B_{\pm}) corners of a rectangular curve $\Gamma_{\infty}^{(4)}$ in the Higgs plane parameterised by (ϕ_x, ϕ_y) . For the case $A_{\pm} = B_{\pm} = \pm L$, the curve $\Gamma_{\infty}^{(4)}$ reduces to a square in \mathbb{R}_{ϕ}^2 , which can be imagined as depicted in the **Figure 2**. Below, we want to re-derive Eq. (2.26)

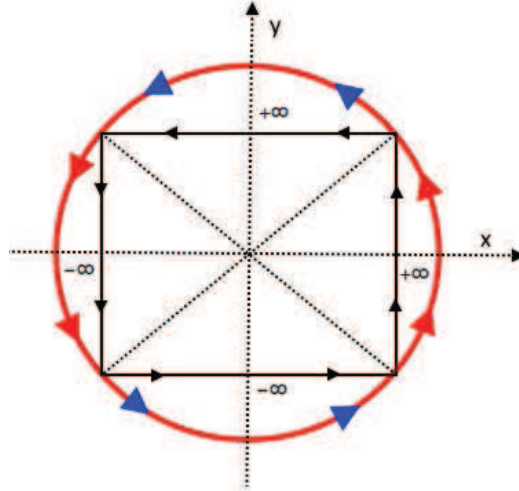


Figure 2: This figure has two interpretations depending on whether we are sitting in $\mathbb{R}_{\mathbf{r}}^2$ or in \mathbb{R}_{ϕ}^2 . From the view of $\mathbb{R}_{\mathbf{r}}^2$, we have a square $\mathcal{C}_{\infty}^{(4)}$ in the x-y plane circumscribed in a circle S^1_r in red color. Under the mapping $\Phi : \mathbf{r} \rightarrow \phi(\mathbf{r})$, this figure can be also interpreted in terms of closed curve $\Gamma_{\infty}^{(4)}$ circumscribed in a circle S^1_{ϕ} in the Higgs plane \mathbb{R}_{ϕ}^2 .

by working directly in the Higgs space \mathbb{R}_{ϕ}^2 . This result, which relies on using some differential geometry tools and topological mappings between $\mathbb{R}_{\mathbf{r}}^2$ and \mathbb{R}_{ϕ}^2 , will be also used later on when we study the third order topological index of the three dimensional BBH lattice model.

Substituting the vector current $J^i(\mathbf{r})$ given by Eq.(2.14) into the relation Eq.(2.12) of the Hamiltonian index in the x-y plane namely

$$Ind(H) = \oint_{\mathcal{C}} \varpi \quad \text{with} \quad \varpi = -\frac{1}{2} \varepsilon_{ij} J^i dx^j \quad (3.1)$$

we obtain a new formula for the index which is completely expressed in the ϕ_x - ϕ_y Higgs plane; it is given by

$$Ind(H) = \oint_{\Gamma} \frac{1}{2\pi |\phi|^2} \varepsilon^{ab} \phi_a d\phi_b \quad (3.2)$$

where now the loop Γ belongs to the ϕ_x - ϕ_y Higgs plane; it is the image of the closed curve \mathcal{C} under the mapping $\phi_a : (x, y) \rightarrow (\phi_x, \phi_y)$. The above equation shows that $\text{Ind}(H)$ has a pole singularity at $|\phi| = 0$ indicating that gapless states live there. To deal with (3.2), which reads also like

$$\text{Ind}(H) = \oint_{\Gamma} \mathcal{B}_a dl^a \quad , \quad dl^a = \varepsilon^{ab} d\phi_b \quad (3.3)$$

with $\mathcal{B}_a = \frac{\phi_a}{2\pi|\phi|^2}$, it is interesting to use new field variables $\varrho = \varrho(x, y)$ and $\vartheta = \vartheta(x, y)$ related to the orders as

$$\begin{aligned} \phi_x &= \varrho \cos \vartheta & , \quad \varrho &= \sqrt{\phi_x^2 + \phi_y^2} \\ \phi_y &= \varrho \sin \vartheta & , \quad \vartheta &= \arctan \frac{\phi_y}{\phi_x} \end{aligned} \quad (3.4)$$

This Higgs field change allows to bring the above index relation into the simple form

$$\text{Ind}(H) = \oint_{\Gamma} \frac{d\vartheta}{2\pi} \quad (3.5)$$

which is easy to deal with. To exhibit the pole singularity, one may also use the complex variables $w = \phi_x + i\phi_y = \varrho e^{i\vartheta}$ and $\bar{w} = \phi_x - i\phi_y = \varrho e^{-i\vartheta}$ and replace $\frac{d\vartheta}{2\pi}$ either by $\frac{dw}{2\pi iw}$ or $-\frac{d\bar{w}}{2\pi i\bar{w}}$; one ends up with the typical relation $\frac{\pm 1}{2\pi i} \oint_{\Gamma} \frac{dw}{w}$ having non zero values for contour Γ surrounding the pole at $w = 0$.

3.2 $\text{Ind}(H)$ in Higgs plane

Clearly, the explicit computation of the integral Eq.(3.5) depends a priori on the shape of the closed curve Γ . If thinking of this loop Γ as an oriented circle with perimeter 2π ; we end up with $\text{Ind}(H) = \pm 1$ depending on the sense of orientation of the circle; one may also get an integer n for the case of an oriented circle with a winding number² n where the perimeter of Γ is $2\pi n$. However, for a loop Γ given by a rectangular —square— cycle made of four edges as in the **Figures 2-3**; one expects to obtain a relation

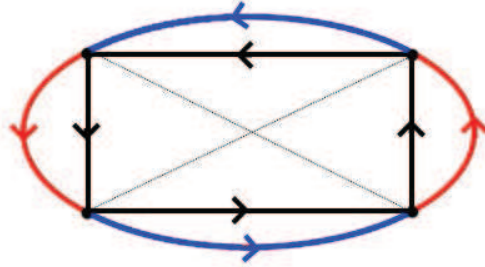


Figure 3: A rectangular loop $\Gamma_{\infty}^{(4)}$ circumscribed into an ellipse in the Higgs plane. One can move continuously from the ellipse to the rectangle by deforming the red and blue arcs of circles into straight line segments.

like in (2.26). In this rectangular case, we have

$$\Gamma_{\infty}^{(4)} = \Gamma_1^+ \cup \Gamma_2^+ \cup \Gamma_1^- \cup \Gamma_2^- \quad (3.6)$$

where the Γ_i^{\pm} 's are as

$$\begin{aligned} \Gamma_1^{\pm} &: B_- \leq \phi_y \leq B_+ \quad ; \quad \phi_x = A_{\pm} \\ \Gamma_2^{\pm} &: A_- \leq \phi_x \leq A_+ \quad ; \quad \phi_y = B_{\pm} \end{aligned} \quad (3.7)$$

² This number may be exhibited in our calculations by considering the general parametrisation $\phi_x = \varrho \cos(n\vartheta)$ and $\phi_y = \varrho \sin(n\vartheta)$ instead of Eq(3.4) corresponding to setting $n = 1$.

where, to fix the ideas, we have assumed $A_- < A_+$ and $B_- < B_+$; but A_\pm and B_\pm can be either positive or negative showing that one can distinguish several cases. From these Γ_i^\pm sets, we learn that they can be also defined by using ratios like

$$\begin{aligned}\Gamma_1^\pm &: \frac{B_-}{A_\pm} \leq \frac{\phi_y}{\phi_x} \leq \frac{B_+}{A_\pm} \\ \Gamma_2^\pm &: \frac{A_-}{B_\pm} \leq \frac{\phi_x}{\phi_y} \leq \frac{A_+}{B_\pm}\end{aligned}\quad (3.8)$$

teaching us that $\frac{\phi_y}{\phi_x} = \arctan \vartheta$ and its inverse $\frac{\phi_x}{\phi_y} = \operatorname{arccot} \vartheta$ are the natural variables to use for describing the square loop $\Gamma_\infty^{(4)}$. Setting $\tan \vartheta_{pq} = \frac{B_q}{A_p}$ and $\cot \vartheta_{pq} = \frac{A_p}{B_q}$, we then have

$$\begin{aligned}\Gamma_1^\pm &: \arctan \frac{B_-}{A_\pm} \leq \vartheta \leq \arctan \frac{B_+}{A_\pm} \\ \Gamma_2^\pm &: \operatorname{arccot} \frac{A_-}{B_\pm} \leq \vartheta \leq \operatorname{arccot} \frac{A_+}{B_\pm}\end{aligned}\quad (3.9)$$

Putting the decomposition (3.6) back into the index formula (3.5) and expanding, we obtain

$$Ind(H) = \int_{\Gamma_1^+} \frac{d\vartheta}{2\pi} + \int_{\Gamma_2^+} \frac{d\vartheta}{2\pi} + \int_{\Gamma_1^-} \frac{d\vartheta}{2\pi} + \int_{\Gamma_2^-} \frac{d\vartheta}{2\pi} \quad (3.10)$$

Then, using (3.9), we end up with

$$\begin{aligned}Ind(H) &= +\frac{1}{2\pi} \left(\arctan \frac{B_+}{A_+} - \arctan \frac{B_-}{A_+} \right) + \frac{1}{2\pi} \left(\operatorname{arccot} \frac{A_+}{B_+} - \operatorname{arccot} \frac{A_-}{B_+} \right) \\ &\quad - \frac{1}{2\pi} \left(\arctan \frac{B_+}{A_-} - \arctan \frac{B_-}{A_-} \right) - \frac{1}{2\pi} \left(\operatorname{arccot} \frac{A_+}{B_-} - \operatorname{arccot} \frac{A_-}{B_-} \right)\end{aligned}\quad (3.11)$$

that coincides precisely with the Fukui formula (2.26); and which we rewrite in the following remarkable factorised form

$$Ind(H) = \frac{1}{2} [sgn(A_+) - sgn(A_-)] \times \frac{1}{2} [sgn(B_+) - sgn(B_-)] \quad (3.12)$$

from which we directly learn the values of $Ind(H)$. This is a topological relation; it depends only on the signature of the values of the Higgs components at spatial infinities; a non zero index requires the non vanishing of each factor in (3.12) showing that $\phi_x(x, y)$ has to change the sign when we go from $x \rightarrow -\infty$ to $x \rightarrow +\infty$ and the same thing should hold for $\phi_y(x, y)$ when going from $y \rightarrow -\infty$ to $y \rightarrow +\infty$. This feature ensures that the closed curve contains inside the pole singularity $|\phi| = 0$ where lives gapless states.

4 Three dimensional BBH model

The topological index of the three dimensional BBH lattice model with full open boundary condition can be determined by studying the ground state properties of a $4+4$ component fermion $\psi = \psi(x, y, z)$ near the Dirac points. Around each one of these points of the 3D model, the fermion ψ is coupled to an external space dependent field doublet $\phi^a = \phi^a(x, y, z)$ — an $O(3)$ Higgs field triplet — with interacting dynamics described by the typical matrix Hamiltonian

$$H = \mathbf{\Lambda}^x k_x + \mathbf{\Lambda}^y k_y + \mathbf{\Lambda}^z k_z + \mathbf{\Omega}^x \phi_x + \mathbf{\Omega}^y \phi_y + \mathbf{\Omega}^z \phi_z \quad (4.1)$$

In this relation, the six hermitian matrices $\mathbf{\Lambda}^i$ and $\mathbf{\Omega}^a$ are 8×8 Dirac matrices realised in terms of three sets of Pauli matrices σ, τ, ρ as follows

$$\begin{aligned}\mathbf{\Lambda}_1 &= \rho_0 \otimes \tau_2 \otimes \sigma_1 & , & \quad \mathbf{\Omega}_1 = \rho_0 \otimes \tau_2 \otimes \sigma_2 \\ \mathbf{\Lambda}_2 &= \rho_0 \otimes \tau_2 \otimes \sigma_3 & , & \quad \mathbf{\Omega}_2 = \rho_0 \otimes \tau_1 \otimes \sigma_0 \\ \mathbf{\Lambda}_3 &= -\rho_2 \otimes \tau_3 \otimes \sigma_0 & , & \quad \mathbf{\Omega}_3 = -\rho_1 \otimes \tau_1 \otimes \sigma_0\end{aligned}\quad (4.2)$$

From these anticommuting matrices that generate a Clifford algebra in 6D, one define as well a chiral operator Γ_7 by the product $\frac{1}{i}\mathbf{\Lambda}_1\mathbf{\Omega}_1\mathbf{\Lambda}_2\mathbf{\Omega}_2\mathbf{\Lambda}_3\mathbf{\Omega}_3$ which reads in terms of the Pauli matrices as follows

$$\Gamma_7 = \rho_3 \otimes \gamma_5 = -\rho_3 \otimes \tau_3 \otimes \sigma_0 \quad (4.3)$$

This operator characterises the corner states which are described by chiral wave functions. From the eigenvalue $H\psi = E\psi$, one learns that ψ has $4 + 4$ components that can be formulated in various ways; for example like the tensor product of three two component spinors $\xi \otimes \zeta \otimes \eta$ as done in [38]; or simply like $\psi = (\boldsymbol{\lambda}, \bar{\boldsymbol{\chi}})^T$ with components

$$\boldsymbol{\lambda} = \begin{pmatrix} \lambda_1 \\ \lambda_2 \\ \lambda_3 \\ \lambda_4 \end{pmatrix}, \quad \boldsymbol{\chi} = \begin{pmatrix} \chi_1 \\ \chi_2 \\ \chi_3 \\ \chi_4 \end{pmatrix} \quad (4.4)$$

The corner states are determined by solving two constraint relations generalising the previous ones in 2D; these are the gapless eigenvalue equation $H\psi = 0$ with

$$H = -i \sum_{j=1}^3 \mathbf{\Lambda}^j \frac{\partial}{\partial x^j} + \mathbf{\Omega}^a \phi_a \quad (4.5)$$

and the chirality condition

$$\Gamma_7 \psi = q_r \psi \quad (4.6)$$

with chiral charge q_r taking either the value $+1$ or -1 and which is fixed by the normality condition of the corner state.

4.1 Integral formula for $\text{Ind}(\mathbf{H})$ in 3D

The Hamiltonian index of the 3D model (4.5) is given by the number of chiral zero modes $N_+ - N_-$ in the ground state. To calculate it, we proceed in a quite similar manner as we have done in 2D model. First, we think about this integer number as the flux of a three dimensional current $J^i = J^i(\mathbf{r})$ like

$$\text{Ind}(H) = \int_S \vec{J} \cdot d\vec{S} = \int_S J^i dS_i \quad (4.7)$$

where $d\vec{S}$ is a vector surface element and \mathcal{S} a closed surface in the x-y-z space $\mathbb{R}^3_{\mathbf{r}}$ traversed by the flux of \vec{J} . We can equivalently express the above relation as follows

$$\text{Ind}(H) = \int_S \varpi \quad (4.8)$$

where now ϖ is 2-form in the real 3D space

$$\varpi = \frac{1}{2} \varpi_{jl} dx^j \wedge dx^l \quad (4.9)$$

related to the vector current J^i like $\varpi_{jl} = \varepsilon_{jli} J^i$ with ε_{jli} the completely antisymmetric Levi-Civita tensor in 3D. By substituting, we obtain

$$\text{Ind}(H) = \frac{1}{2} \int_S \varepsilon_{ijl} J^i dx^j \wedge dx^l \quad (4.10)$$

Having introduced the integral formula for $Ind(H)$, we come now to describe the vector current $J^i = \langle J_7^i \rangle$. It is given by the vacuum expectation value of an axial vector current J_7^i involving the $\mathbf{\Gamma}_7$ matrix as shown on the following expression

$$J^i(\mathbf{r}) = \lim_{\mathbf{r}' \rightarrow \mathbf{r}} \left[\lim_{m \rightarrow 0} \text{tr} \left(\mathbf{\Gamma}_7 \mathbf{\Lambda}^i \frac{1}{m + iH} \right) \delta_3(\mathbf{r} - \mathbf{r}') \right] \quad (4.11)$$

that descends from an underlying quantum field theory description where $J_7^i = \psi^\dagger \mathbf{\Gamma}_7 \mathbf{\Lambda}^i \psi$. The expression of the above current $J^i(\mathbf{r})$ can be also motivated from the two dimensional analysis of section 2; in particular from the study done subsection 2.1. The $J^i(\mathbf{r})$ in Eq(4.11) is nothing but the 3D- extension of the two dimensional current given by Eq(2.13). By comparing the two expressions (4.11) and (2.13), one learns amongst others the two following indicators: First, the 2D- Dirac- delta function $\delta_2(\mathbf{r} - \mathbf{r}')$ in (2.13)—with $\mathbf{r} = (x, y)$ —has been promoted to the three dimensional $\delta_3(\mathbf{r} - \mathbf{r}')$ in (4.11)—with $\mathbf{r} = (x, y, z)$ —. Second, the chiral operator γ_5 in Eq(2.13) has been also promoted to the chiral operator $\mathbf{\Gamma}_7$ of 3D space. Recall that the usual vector space dimension d_v and the spinor dimension d_s are related to each other like $d_s = 2^{d_v}$. So, we have in 2D, we have $d_s = 2^2 = 4$ and then γ_5 is a 4×4 matrix realised in our study as $-\tau_3 \otimes \sigma_0$. In three dimensions, the spinor dimension d_s is equal to $2^3 = 8$; then $\mathbf{\Gamma}_7$ is a 8×8 matrix realised here as $\rho_3 \otimes \gamma_5$. By calculating the trace over the 8×8 matrix product in (4.11) and taking the vanishing mass limit, the above vector current can be expressed in terms of the Higgs field triplet as

$$J^i = \frac{\varepsilon^{abc}}{8\pi |\phi|^3} \varepsilon^{ijl} \phi_a \partial_j \phi_b \partial_l \phi_c \quad (4.12)$$

with $|\phi|^2 = \phi_x^2 + \phi_y^2 + \phi_z^2$. An explicit derivation of Eq.(4.12) is as done in the appendix for the 2D case by following the same steps described there and by using properties of the $\mathbf{\Lambda}^i$ and $\mathbf{\Omega}^a$ matrices (4.2) which are induced by the usual features of Pauli matrices. Putting this 3D vector current J^i back into the relation (4.10), we get the following index formula

$$Ind(H) = \int_{\mathcal{S}} \frac{1}{8\pi |\phi|^2} dS_i \varepsilon^{ijl} \phi_a \partial_j \phi_b \partial_l \phi_c \varepsilon^{abc} \quad (4.13)$$

which can be interpreted as the winding number of the three component Higgs vector ϕ_a field around the closed surface \mathcal{S} .

4.2 Topological index from 3D Higgs space

To determine the $Ind(H)$ value of the Hamiltonian (4.5), we have to perform the integral in Eq.(4.13). To that purpose, we will proceed as follows: As a front matter, we give some useful properties of the relation (4.13) including two examples of shapes of the surface \mathcal{S} appearing in the integral formula of $Ind(H)$; these \mathcal{S} shapes are given by a 2-sphere \mathbb{S}_r^2 at infinity; and a parallelepiped surface $\mathcal{S}_\infty^{(8)}$ respectively as in Eqs.(4.16-4.17). Then, we use results from differential geometry on \mathbb{R}^3 to map Eq(4.13) into an equivalent formula for $Ind(H)$ which is completely expressed in the Higgs space. This new formula is given by

$$Ind(H) = \int_{\Sigma} \frac{1}{8\pi |\phi|^3} \phi_a d\phi_b \wedge d\phi_c \varepsilon^{abc} \quad (4.14)$$

it involves a closed surface Σ to be introduced later on and has a singularity at $|\phi| = 0$. The above formula, to be derived in what follows, plays an important role in our forthcoming calculations.

4.2.1 Irregular boundary surface \mathcal{S}

Roughly speaking, the $\text{Ind}(H)$ defined by Eq.(4.13) is a function of \mathcal{S} ; so the integral formula (4.13) can be defined as

$$\text{Ind}(H) = \mathcal{F}[\mathcal{S}] \quad (4.15)$$

This expression shows that if we want to find the numerical value of $\text{Ind}(H)$, we should specify \mathcal{S} ; unless if the integral (4.13) is independent of the shape of \mathcal{S} . This is precisely what happens in the present case since the $\text{Ind}(H)$ is a topological invariant meaning that $\mathcal{F}[\mathcal{S}] = \mathcal{F}[\mathcal{S}']$ for any \mathcal{S}' related to \mathcal{S} by a continuous transformation. In this topological change the \mathcal{S} is deformed to \mathcal{S}' without affecting the value of $\text{Ind}(H)$. Nevertheless, let us think of the closed surface in (4.13) as given by a big \mathcal{S}_∞ at the boundary of the x-y-z space $\mathbb{R}_{\mathbf{r}}^3$ as in the following Figure. For concreteness, we consider below two \mathcal{S}_∞ and \mathcal{S}'_∞

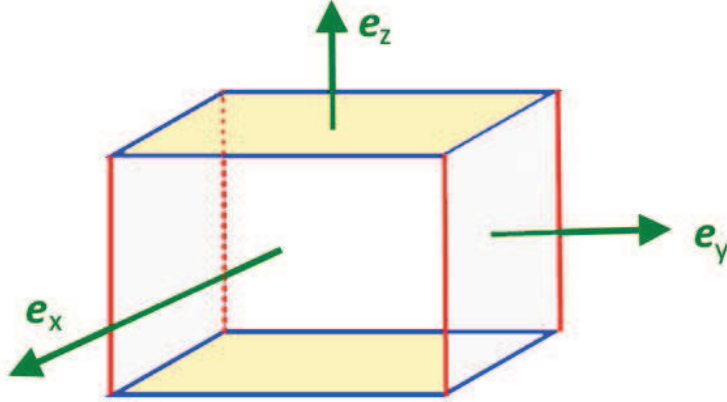


Figure 4: Boundary surface of a parallelepiped in 3D space given by 3+3 faces. These faces bi-intersect on twelve edges and tri-intersect at eight tops. It corresponds to $\mathcal{S}^{(8)}$ from the view of the position space $\mathbb{R}_{\mathbf{r}}^3$ and to the surface $\Sigma^{(8)}$ from the view of \mathbb{R}_{ϕ}^3 .

shapes as follows: (i) \mathcal{S}_∞ given by a 2-sphere $\mathbb{S}_{\mathbf{r}}^2$ with defining equation

$$\mathbb{S}_{\mathbf{r}}^2 : x_\infty^2 + y_\infty^2 + z_\infty^2 = r_\infty^2 \quad (4.16)$$

it is the boundary of the ball \mathcal{V}_∞ with equation $|\mathbf{r}| < r_\infty$; so we have $\mathbb{S}_{\mathbf{r}}^2 = \partial\mathcal{V}$; and (ii) \mathcal{S}'_∞ given by the boundary surface $\mathcal{S}_\infty^{(8)}$ of cube — or in general a regular parallelepiped—. This cubic shape is an interesting situation that concerns 3D matter with full open boundary conditions. In this case, $\mathcal{S}_\infty^{(8)}$ delimits a volume $\mathcal{V}_\infty^{(8)}$ and is given by

$$\mathcal{S}_\infty^{(8)} = (\mathcal{S}_1^+ \cup \mathcal{S}_1^-) \cup (\mathcal{S}_2^+ \cup \mathcal{S}_2^-) \cup (\mathcal{S}_3^+ \cup \mathcal{S}_3^-) \quad (4.17)$$

Concretely $\mathcal{S}_\infty^{(8)}$ has 3 + 3 planar faces \mathcal{S}_i^\pm ; and eight tops with coordinates $(x, y, z) = (\pm L_x, \pm L_y, \pm L_z)$. The planar \mathcal{S}_i^\pm are normal to the x- y- z directions as depicted in the **Figure (4)**; they bi-intersect along the 12 following segments

$$\begin{aligned} C_x^{(p,q)} &\sim \mathcal{S}_y^p \cap \mathcal{S}_z^q \\ C_y^{(p,q)} &\sim \mathcal{S}_x^p \cap \mathcal{S}_z^q \\ C_z^{(p,q)} &\sim \mathcal{S}_x^p \cap \mathcal{S}_y^q \end{aligned} \quad , \quad p, q = \pm \quad (4.18)$$

and tri-intersect at the eight tops

$$\mathbf{T}^{(p,q,s)} \sim \mathcal{S}_1^p \cap \mathcal{S}_2^q \cap \mathcal{S}_3^s \quad , \quad p, q, s = \pm \quad (4.19)$$

This $\mathcal{S}_\infty^{(8)}$ can be also interpreted as describing the boundary of a cube —parallelepiped— circumscribed into a 2-sphere —ellipsoid— as depicted in the **Figure 5**. With this picture, one clearly see that one can pass from $\mathcal{S}_\infty^{(8)}$ to the 2-sphere \mathbb{S}_∞^2 by deforming the planar faces \mathcal{S}_i^\pm into spherical calottes with a square (rectangular) section. The surface shape (4.17) will be used later on when studying the 3D extension of the construction done for the 2D model studied in the previous section.

4.2.2 Deriving the signature Eq.(1.1)

A nice way to determine the $\text{Ind}(\mathbf{H})$ given by Eq.(4.13) is to formulate it directly in the Higgs space \mathbb{R}_ϕ^3 parameterised by (ϕ_x, ϕ_y, ϕ_z) and given by Eq.(4.14). For that, we substitute the two following relations,

$$\begin{aligned} dS_i \varepsilon^{ijl} &= dx^j \wedge dx^l \\ d\phi_a &= \partial_j \phi_a dx^j \end{aligned} \quad (4.20)$$

back into Eq.(4.13) to end up exactly with (4.14). But, in this index relation, the Σ is a closed surface in the Higgs space — Σ is contained in \mathbb{R}_ϕ^3 —; it is given by the correspondence $\Phi : \mathcal{S} \rightarrow \Sigma$ mapping the real surface \mathcal{S} of the x-y-z space $\mathbb{R}_\mathbf{r}^3$ into the surface Σ belonging ϕ_x - ϕ_y - ϕ_z space. Under this correspondence, each point $\mathbf{r} = (x, y, z)$ in the 3D position space $\mathbb{R}_\mathbf{r}^3$ gets mapped into a point $\phi = (\phi_x, \phi_y, \phi_z)$ in the 3D Higgs space \mathbb{R}_ϕ^3 . Notice that because of this mapping, several relations in $\mathbb{R}_\mathbf{r}^3$ can be also mapped into corresponding ones in \mathbb{R}_ϕ^3 . Below, we give two interesting examples respectively dealing with Eq.(4.7) and Eqs.(4.16-4.17). The first example concerns the flux formula (4.7) whose homologue in the Higgs space is obtained by setting

$$d\sigma^a = \frac{1}{2} \varepsilon^{abc} d\phi_b \wedge d\phi_c \quad (4.21)$$

into Eq.(4.14); this substitution allows to bring the flux formula into the interesting form

$$\text{ind}(H) = \int_\Sigma \mathcal{B}_a d\sigma^a = \int_\Sigma \vec{\mathcal{B}} \cdot d\vec{\sigma} \quad (4.22)$$

with vector field $\mathcal{B}_a = \frac{\phi_a}{4\pi|\phi|^3}$. This index relation, which describes the flux of \mathcal{B}_a through Σ , is remarkable in the sense it can be also put in correspondence with the well known Gauss theorem concerning the electrostatic field of Coulomb theory. The second example concerns the surface \mathcal{S} and its image Σ ; for \mathcal{S}_∞ given by the 2-sphere $\mathbb{S}_\mathbf{r}^2$ of Eq.(4.16), it is associated a 2-sphere $\Sigma_\infty = \mathbb{S}_\phi^2$ given by

$$\mathbb{S}_\phi^2 : \phi_{x\infty}^2 + \phi_{y\infty}^2 + \phi_{z\infty}^2 = \phi_\infty^2 \quad (4.23)$$

Similarly, for the $\mathcal{S}_\infty^{(8)}$ given by (4.17), we have the corresponding Higgs space surface

$$\Sigma_\infty^{(8)} = (\Sigma_1^+ \cup \Sigma_1^-) \cup (\Sigma_2^+ \cup \Sigma_2^-) \cup (\Sigma_3^+ \cup \Sigma_3^-) \quad (4.24)$$

it has 3 + 3 faces Σ_i^\pm normal to the ϕ_i - directions in the Higgs space; twelve edges

$$\mathcal{C}_j^{(p,q)} \sim \varepsilon_{lij} \Sigma_i^p \cap \Sigma_j^q \quad (4.25)$$

and eight tops

$$\mathcal{T}^{(p,q,s)} \sim \Sigma_1^p \cap \Sigma_2^q \cap \Sigma_3^s \quad , \quad p, q, s = \pm \quad (4.26)$$

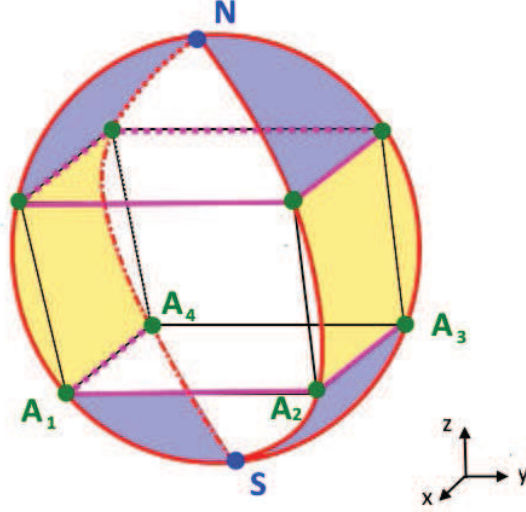


Figure 5: A boundary surface space of a cube circumscribed inside a 2-sphere \mathbb{S}^2 . This picture holds both for the $\mathcal{S}_\infty^{(8)}$ of the position space and its image $\Sigma_\infty^{(8)}$ living in the Higgs space.

with coordinates $(\phi_x, \phi_y, \phi_z) = (A_\pm, B_\pm, C_\pm)$. Here also $\Sigma_\infty^{(8)}$ has an interpretation in terms of a cube —parallelepiped— circumscribed into the 2-sphere \mathbb{S}_ϕ^2 —ellipsoid— as depicted in the **Figure 5**. In this realisation, the two parallel faces Σ_x^\pm are normal to ϕ_x -direction and are located at $\phi_{x \rightarrow \pm\infty} = \phi_{x_\pm\infty}$; a similar thing is valid for Σ_2^\pm and Σ_3^\pm respectively normal to ϕ_y - and ϕ_z - directions. For later use notice that the planar faces Σ_i^\pm can be also defined as cross products of edges. Denoting the 12 edges of the cube —parallelepiped—like

$$\begin{aligned} \mathcal{C}_x^{(p,q)} &: A_- \leq \phi_x \leq A_+ \quad , \quad (\phi_y, \phi_z) = (B_p, C_q) \\ \mathcal{C}_y^{(p,q)} &: B_- \leq \phi_y \leq B_+ \quad , \quad (\phi_x, \phi_z) = (A_p, C_q) \\ \mathcal{C}_z^{(p,q)} &: C_- \leq \phi_z \leq C_+ \quad , \quad (\phi_x, \phi_y) = (A_p, B_q) \end{aligned} \quad (4.27)$$

and the union of the four upper (resp. lower) edges of the face Σ_3^+ (resp. Σ_3^-) as

$$\mathcal{P}_{xy}^{(q)} = \mathcal{C}_x^{(+,q)} \cup \mathcal{C}_y^{(+,q)} \cup \mathcal{C}_x^{(-,q)} \cup \mathcal{C}_y^{(-,q)} \quad (4.28)$$

we can think of $\Sigma_\infty^{(8)}$ as the union $\Sigma_L \cup (\Sigma_3^+ \cup \Sigma_3^-)$ with Σ_L standing for the lateral surface $(\Sigma_1^+ \cup \Sigma_1^-) \cup (\Sigma_2^+ \cup \Sigma_2^-)$ of a cylinder with rectangular cross section. Moreover, using the relation $\Sigma_L \sim \mathcal{C}_z \times \mathcal{P}_{xy}$, we end up with

$$\Sigma_\infty^{(8)} \sim (\mathcal{C}_z \times \mathcal{P}_{xy}) \cup (\Sigma_3^+ \cup \Sigma_3^-) \quad (4.29)$$

With these data on the surface \mathcal{S}_∞ and its image Σ_∞ in the Higgs space, we are now in position to determine the value of $\text{Ind}(\mathbf{H})$ by using the Higgs space formula (4.22). For the spherical choice $\Sigma_\infty = \mathbb{S}_\phi^2$, it is interesting to use following change of field variable,

$$\begin{aligned} \phi_x &= \phi \sin \vartheta \cos \varphi \\ \phi_y &= \phi \sin \vartheta \sin \varphi \\ \phi_z &= \phi \cos \vartheta \end{aligned} \quad (4.30)$$

to perform the integral in (4.22). From this change, we learn the associated quantities $\varrho^2 = \phi_x^2 + \phi_y^2$ and $\phi^2 = \varrho^2 + \phi_z^2$ as well as

$$\tan \varphi = \frac{\phi_y}{\phi_x} \quad , \quad \cos \vartheta = \frac{\phi_z}{\phi} \quad , \quad \tan^2 \vartheta = \frac{\varrho^2}{\phi^2} \quad (4.31)$$

Putting the field change (4.30) back into Eq.(4.22), we obtain

$$Ind(H) = \pm \frac{1}{4\pi} \int_{\Sigma_\infty} \sin \vartheta d\vartheta d\varphi \quad (4.32)$$

giving ± 1 ; thanks to the radial symmetry of \mathcal{B}_a . For the cartesian shape $\Sigma_\infty^{(8)}$ given by (4.24), it is interesting to still use the (ϑ, φ) angles to compute the index $\int_{\Sigma_\infty^{(8)}} \mathcal{B}_a d\sigma^a$ which, as shown on (4.29), decomposes as the sum of three terms like $\mathcal{J}_0 + \mathcal{J}_+ + \mathcal{J}_-$ with $\mathcal{J}_{0,\pm}$ respectively given by

$$\mathcal{J}_0 = \int_{\mathcal{C}_z \times \mathcal{P}_{xy}} \mathcal{B}_a d\sigma^a \quad , \quad \mathcal{J}_\pm = \int_{\Sigma_3^\pm} \mathcal{B}_a d\sigma^a \quad (4.33)$$

Straightforward calculations lead to

$$\begin{aligned} \mathcal{J}_0 &= \frac{\mathcal{I}_{\mathcal{P}_{xy}}}{2} (\cos \vartheta_+ - \cos \vartheta_-) \\ \mathcal{J}_+ &= \frac{\mathcal{I}_{\mathcal{P}_{xy}}}{2} (1 - \cos \vartheta_+) \\ \mathcal{J}_- &= \frac{\mathcal{I}_{\mathcal{P}_{xy}}}{2} (\cos \vartheta_- + 1) \end{aligned} \quad (4.34)$$

with $\vartheta_\pm = \arccos \frac{C_\pm}{\phi}$ and $\mathcal{I}_{\mathcal{P}_{xy}}$ as follows

$$\mathcal{I}_{\mathcal{P}_{xy}} = \frac{1}{4} [\text{sgn}(A_+ B_+) + \text{sgn}(A_- B_-)] - \frac{1}{4} [\text{sgn}(A_+ B_-) + \text{sgn}(A_- B_+)] \quad (4.35)$$

The sum of the three relations of Eq.(4.34) gives exactly $\mathcal{I}_{\mathcal{P}_{xy}}$; it looks as it doesn't depend on $\text{sgn}(C_\pm)$; and, according to (3.12), it is an integer. A way to interpret the absence of $\text{sgn}(C_\pm)$ is because of the choice we have used in our calculation namely $\text{sgn}(C_-) = -\text{sgn}(C_+) = -1$. To implement, the contribution of $\text{sgn}(C_\pm)$, we think of the above index as given by

$$Ind(H) = \frac{\mathcal{I}_{\mathcal{P}_{xy}}}{2} [\text{sgn}(C_+) - \text{sgn}(C_-)] \quad (4.36)$$

by setting $\text{sgn}(C_+) = 1$, one recovers (4.35). This relation can be also motivated by its factorised form (3.12) and cyclic symmetry properties allowing to determine $\mathcal{I}_{\mathcal{P}_{yz}}$ and $\mathcal{I}_{\mathcal{P}_{zx}}$ from $\mathcal{I}_{\mathcal{P}_{xy}}$. Expanding the above generalisation, we get

$$\begin{aligned} Ind(H) &= +\frac{1}{8} [\text{sgn}(A_+ B_+ C_+) + \text{sgn}(A_- B_- C_+)] \\ &+ \frac{1}{8} [\text{sgn}(A_+ B_- C_-) + \text{sgn}(A_- B_+ C_-)] \\ &- \frac{1}{8} [\text{sgn}(A_+ B_- C_+) + \text{sgn}(A_- B_+ C_+)] \\ &- \frac{1}{8} [\text{sgn}(A_+ B_+ C_-) + \text{sgn}(A_- B_- C_-)] \end{aligned} \quad (4.37)$$

having eight contributions in one to one correspondence with the corners of the cube —parallelepiped— with tops (A_\pm, B_\pm, C_\pm) . In the end notice that, like for (3.12) of the 2D model, this topological formula factorises as follows,

$$\begin{aligned} Ind(H) &= \frac{1}{2} [\text{sgn}(A_+) - \text{sgn}(A_-)] \times \\ &\frac{1}{2} [\text{sgn}(B_+) - \text{sgn}(B_-)] \times \\ &\frac{1}{2} [\text{sgn}(C_+) - \text{sgn}(C_-)] \end{aligned} \quad (4.38)$$

and showing that here also that $\text{sgn}(\phi_a)$ has to change its polarity when we go from minus infinity to plus infinity in order to have a non trivial value of the index. For a non trivial value of $\text{Ind}(\text{H})$, the surface Σ has to englobe the pole singularity at $|\phi| = 0$.

5 Conclusion and comments

In this paper, we studied the topological properties of the three dimensional BBH lattice model falling into the DBI class in the AZ periodic table with reflection symmetries. First, we revisited the 2D model and re-derived the topological index $\text{Ind}(\text{H}_{2D})$ of this theory by using topological mapping from the real x-y plane \mathbb{R}_x^2 into the ϕ_x - ϕ_y Higgs plane \mathbb{R}_ϕ^2 . Then, we investigated the topological $\text{Ind}(\text{H}_{3D})$ of the 3D theory and calculated its expression in terms of the limit values of the Higgs field triplet at space infinity. The topological index formula given by (4.37) can remarkably factorise like in (4.38). Our method revealed that the results obtained for 2D, given by (2.26;3.12); and their homologue derived for 3D, correspond to leading terms of a general DBI topological index formula given by

$$\text{Ind}(\text{H}_{ND}) = \prod_{a=1}^N \frac{1}{2} [\text{sgn}(A_{+a}) - \text{sgn}(A_{-a})] \quad (5.1)$$

where $(A_{\pm i})_{1 \leq i \leq N}$'s stand for the values at space infinities of a N- component Higgs field multiplet; i.e $\phi = (\phi_a)_{1 \leq a \leq N}$. Non zero topological index requires A_{+a} and A_{-a} to have opposite signs. The above relation depends only on the signatures of the A_{p_a} values with $p_a = \pm 1$; and can be also expressed in other different ways: for example like

$$\text{Ind}(\text{H}_{ND}) = \prod_{a=1}^N \sum_{p_a = \pm} \frac{p_a}{2} \text{sgn}(A_{p_a}) \quad (5.2)$$

By setting $\text{sgn}(A_{\pm a}) = (-)^{\xi_{\pm a}}$ with integer $\xi_{\pm a} = 0, 1 \bmod 2$, the above index formula can be re-expressed as follows

$$\text{Ind}(\text{H}_{ND}) = \prod_{a=1}^N \frac{1}{2} (e^{i\pi\xi_{+a}} - e^{i\pi\xi_{-a}}) \quad (5.3)$$

which, up to a sign, reads like $\frac{1}{2^N} \prod_{a=1}^N (1 - e^{i\pi\xi_a})$ with ξ_a given by the difference $\xi_{+a} - \xi_{-a}$. Like for 2D and 3D, a non zero value of the Hamiltonian index in higher dimensions requires that the boundary hypersurface Σ contains in its inside the pole singularity $|\phi| = 0$.

6 Appendices

Here, we give two appendices A and B aiming some technical details, which for simplicity of the presentation and also for the chain of ideas, have been omitted in the heart of the paper. In appendix A, we give some useful information on the Hamiltonians (2.1-2.6) and make a comment regarding the vector field (ϕ_x, ϕ_y, ϕ_z) . In appendix B, we give explicit details regarding the derivation of the 2D topological current of Eq.(2.14) used in sections 3 and 4.

6.1 Appendix A: More on Hamiltonian (2.1)

The 3D- extension of the two dimensional BBH lattice Hamiltonian model with full open boundary condition reads in reciprocal space as follows

$$\begin{aligned} \mathbf{H}_{lat} = & +t_x (\sin k_x) \mathbf{\Lambda}^x + (\Delta_x + t_x \cos k_x) \mathbf{\Omega}^x \\ & +t_y (\sin k_y) \mathbf{\Lambda}^y + (\Delta_y + t_y \cos k_y) \mathbf{\Omega}^y \\ & +t_z (\sin k_z) \mathbf{\Lambda}^z + (\Delta_z + t_z \cos k_z) \mathbf{\Omega}^z \end{aligned} \quad (6.1)$$

where $\mathbf{\Lambda}^i$ and $\mathbf{\Omega}^i$ are hermitian 8×8 matrices given by Eqs(4.2) and where Δ_i and t_i are hopping parameters: intra and extra unit cells. For simplicity of the presentation given below, we set $t_x = t_y = t_z = 1$; the reduction down to 2D can be obtained by cutting the z-direction ($t_z = \Delta_z = 0$) and thinking of the remaining reduced $\mathbf{\Lambda}^i$ and $\mathbf{\Omega}^i$ as hermitian 4×4 matrices with realisation as in Eqs(2.7). Notice that by setting $\Theta_i = (\Delta_i + \cos k_i)$ with $i = x, y, z$, we can express the above lattice Hamiltonian \mathbf{H}_{lat} as a matrix function of the 3 momentum variables (k_x, k_y, k_z) and the three $(\Theta_x, \Theta_y, \Theta_z)$; that is

$$\mathbf{H}_{lat} = \mathbf{H}_{lat}(k_x, k_y, k_z; \Theta_x, \Theta_y, \Theta_z). \quad (6.2)$$

However as $\Theta_i = \Theta(k_i)$, the lattice Hamiltonian is then a function $\mathbf{H}_{lat}(k_x, k_y, k_z)$; so the symmetry constraints (2.2) and (2.3) apply as well to $\mathbf{H}_{lat} = \sum_i (\mathbf{\Lambda}^i \sin k_i + \mathbf{\Omega}^i \Theta_i)$. To see the relationship between this \mathbf{H}_{lat} and (2.1); we calculate the eight energy eigenvalues of \mathbf{H}_{lat} ; they are nicely obtained by computing \mathbf{H}_{lat}^2 which turns out to be proportional to the identity matrix $I_{8 \times 8}$; that is $\mathbf{H}_{lat}^2 = E_{lat}^2 I_{8 \times 8}$. This feature leads to the two following E_{lat}^\pm energies with multiplicity of order 4,

$$E_{lat}^\pm = \pm \sqrt{\sum_{i=x,y,z} [\sin^2 k_i + (\Delta_i + \cos k_i)^2]}. \quad (6.3)$$

The gap energy is determined by looking for the minimal value of $(E_{lat}^+)_{\min}$; it is obtained by solving the vanishing of two following sets of equations:

$$(I) : \sin k_i = 0 \quad , \quad (II) : \Delta_i + \cos k_i = 0. \quad (6.4)$$

While the set (II) shows that for $|\Delta_i| > 1$, the system is gapped; the first set teaches us interesting information. First, it has eight solutions that can be expressed like $k_i^* = n_i \pi$ with $n_i = 0, 1 \bmod 2$. Therefore, given a fix point $(k_x^*, k_y^*, k_z^*) = (n_x \pi, n_y \pi, n_z \pi)$ with some integers (n_x, n_y, n_z) , the momentum vector k_i around the k_i^* expands as follows

$$k_i \simeq k_i^* + k'_i = n_i \pi + k'_i \quad (6.5)$$

where k'_i is a small deviation; that is $|\mathbf{k}'|/|\mathbf{k}^*| \ll 1$. Second, putting this change back into in Eq(6.1), we can approximate the lattice Hamiltonian $\mathbf{H}_{lat}(\mathbf{k})$ near \mathbf{k}^* like $H_{n_x, n_y, n_z}(\mathbf{k}') + O(\mathbf{k}'^2)$ with

$$H_{n_x, n_y, n_z} = \sum_{i=x,y,z} (-)^{n_i} [k'_i \mathbf{\Lambda}^i + \varphi'_{n_i} \mathbf{\Omega}^i] \quad (6.6)$$

with $\varphi'_{n_i} = 1 + \Delta_i \cos(n_i \pi)$. For example, near the point (k_x^*, k_y^*, k_z^*) given by the origin $(0, 0, 0)$, we have the Hamiltonian $H_{0,0,0} = \sum_i [k'_i \mathbf{\Lambda}^i + \varphi'_i \mathbf{\Omega}^i]$ with $\varphi'_i = (1 + \Delta_i)$. Quantum fluctuations are described by realising the momentum deviations k'_i in terms of the operators $k'_x = -i \frac{\partial}{\partial x'}$ and so on. Topological properties are described by promoting the above φ'_i 's space coordinate dependent Higgs $\phi_i(\mathbf{r}')$ with $\mathbf{r}' = (x', y', z')$. By dropping out the primes from \mathbf{k}' and \mathbf{r}' ; one recovers amongst others Eqs. (2.1-2.6).

6.2 Appendix B: Derivation of Eq.(2.14)

Here, we give a rapid sketch of the derivation of the topological current $J^i(\mathbf{r})$ given by Eq.(2.14) by starting from the following definition of the axial current using Pauli-Villars regularisation parameter M ,

$$J^i(\mathbf{r}) = \lim_{\mathbf{r}' \rightarrow \mathbf{r}} \lim_{m \rightarrow 0} \lim_{M \rightarrow \infty} \text{tr} \left[\gamma_5 \Lambda^i \left(\frac{1}{iH + m} - \frac{1}{iH + M} \right) \delta_2(\mathbf{r} - \mathbf{r}') \right]. \quad (6.7)$$

Strictly speaking, this relation involves four operations that we have to perform in order to put $J^i(\mathbf{r})$ into the remarkable form (2.14) used in the paper. These operations are given by the matrix trace $\text{tr}(\dots)$ which we have to calculate; and moreover three limits namely $\lim_{M \rightarrow \infty}$ and $\lim_{m \rightarrow 0}$ as well as $\lim_{\mathbf{r}' \rightarrow \mathbf{r}}$ that we have to perform as well. In our present situation, the limit $\lim_{M \rightarrow \infty}$ is trivial and the term $1/(iH + M)$ in (6.7) can be dropped out. So, we are left with the basic term that we express like

$$J^i(\mathbf{r}) = \lim_{\mathbf{r}' \rightarrow \mathbf{r}} \lim_{m \rightarrow 0} \text{tr} \left[\gamma_5 \Lambda^i \left(\frac{m - iH}{H^2 + m^2} \right) \delta_2(\mathbf{r} - \mathbf{r}') \right]. \quad (6.8)$$

To proceed, we first perform the $\lim_{\mathbf{r}' \rightarrow \mathbf{r}}$ by substituting the Dirac- delta function $\delta_2(\mathbf{r} - \mathbf{r}')$ by its expression as an integral over the plane waves $e^{i\mathbf{k} \cdot (\mathbf{r} - \mathbf{r}')}$ and think of H like a differential operator $-i\Lambda^j \partial_j + \Omega^a \phi_a$; this leads to put $J^i(\mathbf{r})$ in the form $\lim_{m \rightarrow 0} \mathcal{J}^i(\mathbf{r}; m)$ with

$$\mathcal{J}^i(\mathbf{r}; m) = \int_{R^2} \frac{d^2 \mathbf{k}}{(2\pi)^2} \text{tr} \left[\gamma_5 \Lambda^i e^{-i\mathbf{k} \cdot \mathbf{r}} \left(\frac{m - iH}{H^2 + m^2} \right) e^{i\mathbf{k} \cdot \mathbf{r}} \right] \quad (6.9)$$

We will show later on that the $\lim_{m \rightarrow 0}$ is also trivial here; but let us keep it for a moment and kill it at proper time. The remaining steps to do are technical and rely on some key ingredients; in particular the two following ones that we want to comment on as they concern crucial stages: (i) The way to deal with the inverse operator $\frac{1}{H^2 + m^2}$ appearing in (6.9) as it hides a difficulty that we have to overcome in order to get a simple expression of the current. The point is that the quantity $e^{-i\mathbf{k} \cdot \mathbf{r}} H^2 e^{i\mathbf{k} \cdot \mathbf{r}}$, which is equal to $\mathbf{k}^2 + \phi^2 - i\Lambda^j \Omega^a \partial_j \phi_a + \mathcal{O}_2$ with $\mathcal{O}_2 = -\nabla^2 - 2i(\mathbf{k} \cdot \nabla)$, involves the field matrix $\Lambda^j \Omega^a \partial_j \phi_a$. After substituting, we can put $e^{-i\mathbf{k} \cdot \mathbf{r}} (H^2 + m^2)^{-1} e^{i\mathbf{k} \cdot \mathbf{r}}$ as the product of $(\mathbf{k}^2 + \phi^2 + m^2)^{-1}$ with $1/(I + \Theta_m)$ where Θ_m is roughly given by the matrix $-i\Lambda^j \Omega^a \partial_j \phi_a$ divided by the number $(\mathbf{k}^2 + \phi^2 + m^2)$; that is

$$\Theta_m = \frac{-i\Lambda^j \Omega^a \partial_j \phi_a + \mathcal{O}_2}{\mathbf{k}^2 + \phi^2 + m^2} \quad (6.10)$$

In other words, the term $(H^2 + m^2)^{-1}$ in (6.9) involves the fraction $1/(I + \Theta_m)$ having matrices in the denominator. But this dependence poses a problem when coming to the explicit calculation of the matrix trace in (6.9). Hopefully, one can use perturbation theory methods to replace $1/(I + \Theta_m)$ by its expansion in Θ - powers given by $I - \Theta_m +$ higher powers. This demands however assuming $|\Theta|$ small which is equivalent the condition $|\partial_j \phi_a| \ll |\phi|^2$ requiring a slow variation of the field gradient $\nabla \phi$ with respect to the variation of ϕ . (ii) The second key ingredient we want to comment comes from the computation of matrix traces like $\text{tr}[\gamma_5 \Lambda^i(X)]$ where X is given by products type $\Pi_{n=1}^N \Lambda^{i_n} \Pi_{n'=1}^{N'} \Omega^{j_{n'}}$ and having in mind that $\text{tr}(\Lambda^i) = \text{tr}(\Omega^i) = 0$ and $\text{tr}(I_4) = 4$. However, traces of the form $\text{tr}[\gamma_5 \Lambda^i(X)]$ have non vanishing values except for $X \equiv X_i$ proportional to the product $\varepsilon_{ij} \Lambda^j \times (\Omega^k \Omega'^{\varepsilon_{kl}})$. In this regards, recall that $\gamma_5 = -\Lambda^x \Omega^x \Lambda^y \Omega^y$ and so $\text{tr}(\gamma_5 \Lambda^x \Lambda^y \Omega^x \Omega^y) = 4$. This means that the $\frac{m - iH}{H^2 + m^2}$ in (6.9) should contribute by X_i given by the product of three matrices: one appropriate Λ and two Ω 's. This feature rules out the term $\frac{m}{H^2 + m^2}$ in (6.9) leaving only $\frac{-iH}{H^2 + m^2}$. This is because the monomials $[\Theta_m]^n$ in the expansion of $1/(I + \Theta_m)$ produces terms like $(\Lambda^j \Omega^a)^n$ while a non vanishing trace requires terms as $\varepsilon_{ij} \Lambda^j \times (\Omega^a \Omega^b \varepsilon_{ab})$. By taking the limit $\lim_{m \rightarrow 0}$, we can put (6.9) into the following factorised form

$$\mathcal{J}^i(\mathbf{r}) = \text{tr}(\gamma_5 \Lambda^i \Omega^a \Lambda^j \Omega^b) \times \phi_a \partial_j \phi_b \times \int_{R^2} \frac{d^2 \mathbf{k}}{(2\pi)^2} \frac{1}{(\mathbf{k}^2 + \phi^2)^2} \quad (6.11)$$

where we have dropped out irrelevant terms such as those involving the \mathcal{O}'_i s. By substituting the trace $\text{tr}(\gamma_5 \Lambda^i \Omega^a \Lambda^j \Omega^b)$ by its value $4\epsilon^{ij}\epsilon^{ab}$; then performing the change $\mathbf{q} = \mathbf{k}/|\phi|$ and using the integral result $\int_0^\infty \frac{\rho d\rho}{(1+\rho^2)^2} = \frac{1}{2}$, we end up with the following expression

$$\mathcal{J}^i(\mathbf{r}) = \frac{1}{2} \times \frac{1}{2\pi} \times \frac{4}{|\phi|^2} \epsilon^{ij} \phi_a \partial_j \phi_b \epsilon^{ab} \quad (6.12)$$

which is precisely Eq(2.14).

Acknowledgement 1: *The authors would like to acknowledge "Académie Hassan II des Sciences et Techniques-Morocco" for financial support. L. B. Drissi acknowledges the Alexander von Humboldt Foundation for financial support via the Georg Forster Research Fellowship for experienced scientists (Ref 3.4 - MAR - 1202992).*

References

- [1] A. Altland and M. R. Zirnbauer, Physical Review B 55,1142 (1997).
- [2] A. P. Schnyder, S. Ryu, A. Furusaki, and A. W. W. Ludwig, Physical Review B 78, 195125 (2008).
- [3] W. A. Benalcazar, B. A. Bernevig, and T. L. Hughes, Science 357, 61 (2017).
- [4] W. A. Benalcazar, B. A. Bernevig, and T. L. Hughes, Physical Review B 96, 245115 (2017).
- [5] F. Schindler, A. M. Cook, M. G. Vergniory, Z. Wang, S. S. P. Parkin, B. A. Bernevig, and T. Neupert, Sci. Adv. 4, eaat0346 (2018).
- [6] Z. Song, Z. Fang, and C. Fang, Phys. Rev. Lett. 119, 246402 (2017).
- [7] M. Serra-Garcia, V. Peri, R. Süssstrunk, O. R. Bilal, T. Larsen, L. G. Villanueva, and S. D. Huber, Nature 555, 342-345 (2018).
- [8] C. W. Peterson, W. A. Benalcazar, T. L. Hughes, and G. Bahl, Nature 555, 346-350 (2018).
- [9] J. Noh, W. A. Benalcazar, S. Huang, M. J. Collins, K. P. Chen, T. L. Hughes, and M. C. Rechtsman, Nat. Photon. 12, 408-415 (2018).
- [10] S. Imhof. et al, Nat. Phys. 14, 925-929 (2018).
- [11] H. Xue, Y. Yang, F. Gao, Y. Chong, and B. Zhang, Nat. Mater. 18, 108-112 (2019).
- [12] X. Ni, M. Weiner, A. Alù, and A. B. Khanikaev, Nat. Mater. 18, 113-120 (2019).
- [13] M. Serra-Garcia, R. Süssstrunk, and S. D. Huber, Phys. Rev. B 99, 020304(R) (2019).
- [14] F. Schindler. et al, Nat. Phys. 14, 918-924 (2018).
- [15] Rui Chen, Chui-Zhen Chen, Jin-Hua Gao, Bin Zhou, Dong-Hui Xu, Higher-Order Topological Insulators in Quasicrystals, arXiv:1904.09932.
- [16] M. Ezawa, Phys. Rev. Lett. 120 026801 (2018).
- [17] J. Langbehn, Y. Peng, L. Trifunovic, F. von Oppen, and P. W. Brouwer, Phys. Rev. Lett. 119, 246401 (2017).

- [18] M. Serra-Garcia, V. Peri, R. Süsstrunk, O. R. Bilal, T. Larsen, L. G. Villanueva, and S. D. Huber, *Nature*. 2018 Mar 15; 555 (7696) 342-345.
- [19] H. Xue, Y. Yang, G. Liu, F. Gao, Y. Chong, and B. Zhang, *Phys. Rev. Lett.* 122, 244301 (2019).
- [20] H. Xue, Y. Yang, F. Gao, Y. Chong, and B. Zhang, *Nat. Mater.* 18, 108-112 (2019).
- [21] S. Ono, and H. Watanabe, *Phys. Rev. B* 98, 115150 (2018).
- [22] A. P. Schnyder, S. Ryu, A. Furusaki, and A. W. W. Ludwig, *Phys. Rev. B* 78, 195125 (2008).
- [23] M. Z. Hasan and C. L. Kane, *Rev. Mod. Phys.* 82, 3045 (2010).
- [24] R. Kennedy and M. R. Zirnbauer, *Commun. Math. Physics* 342(3) 909 (2016).
- [25] Z. Wang, X-L. Qi, and S-C Zhang, *Phys. Rev. Lett* 105 256803 (2010).
- [26] A. Karch, *Phys. Rev. Lett.* 103, 171601 (2009).
- [27] G. Rosenberg and M. Franz, *Phys. Rev. B* 82, 035105 (2010).
- [28] H. Li, and K. Sun, *Phys Rev Lett* 124 036401 (2020).
- [29] E. P. L. van Nieuwenburg and S. D. Huber, *Phys. Rev. B* 90, 075141 (2014).
- [30] D. Linzner, L. Wawer, F. Grusdt, and M. Fleischhauer, *Phys. Rev. B* 94, 201105(R) (2016).
- [31] C.-E. Bardyn, L. Wawer, A. Altland, M. Fleischhauer, and S. Diehl, *Phys. Rev. X* 8, 011035 (2018)
- [32] J-H. Zheng and W. Hofstett, *Phys Rev B* 97 195434 (2018).
- [33] W. P. Su, J. R. Schrieffer, and A. J. Heeger. Solitons in polyacetylene. *Phys. Rev. Lett.* 42, 1698–1701 (1979)
- [34] T. Fukui, *Phys. Rev. B* 99, 165129 (2019).
- [35] R. Jackiw and P. Rossi, *Nucl. Phys. B* 190 (1981).
- [36] Y. Takane, *J. Phys. Soc. Jpn.* 88, 094712 (2019).
- [37] R. Okugawa, S. Hayashi, and T. Nakanishi, *Phys. Rev. B* 100, 235302, (2019).
- [38] L. B. Drissi et al; A coupled fermion-Higgs model for third order topological insulators, submitted.
- [39] T. Fukui and T. Fujiwara, *J. Phys. Soc. Jpn.* 79, 033701 (2010).
- [40] T. Fujiwara and T. Fukui, *Phys. Rev. D* 85, 125034 (2012).
- [41] K. Shiozaki, T. Fukui, and S. Fujimoto, *Phys. Rev. B* 86, 125405 (2012).
- [42] T. Fukui and T. Fujiwara, *Phys. Rev. B* 96, 205404 (2017).